Model predictive control and trajectory optimization of large vehicle-manipulators

1st Balint Varga, 2nd Selina Meier, 3rd Stefan Schwab
Control in Information Technology
FZI, Research Center for Information Technology
Karlsruhe, Germany
varga@fzi.de, meier@fzi.de, schwab@fzi.de

4th Sören Hohmann
Institute of Control Systems
Karlsruhe Institute for Technology
Karlsruhe, Germany
soeren.hohmann@kit.edu

***Abstract*—In this paper, a model predictive control (MPC) is developed for on- and off-road mid-sized heavy duty vehicle-manipulator systems with a hydraulic working arm. The proposed concept for the control model is also new in the sense of working only within a local reference coordinate-system relative to the reference trajectory (so-called Frenét-System). The control model only needs the errors to the reference trajectory. In contrast to other state-of-the-art approaches, there is no global localization method necessary. The control model is kept as simple as possible, to allow real-time motion prediction of the real system. For this reason, a kinematic model is used in the MPC which consists of a bicycle model and a planar robotic arm with two control variables. The dynamics of the overall system are considered as optimization constraints, assuming that the optimized system inputs and states are kinetically and dynamically feasible. Through this control method, the dual-trajectories are also optimized and they provide smooth motions for the overall system. The underlying control of the robotic arm is realized with a proportional–integral–derivative (PID) controller with feedback linearisation and gravity compensation. The control algorithm is tested and validated in a MATLAB/Simulink simulation environment.**

***Index Terms*—modeling, vehicle-manipulator control, hydraulics, predictive control, mobile manipulator**

I. Introduction

One of the largest fields of robotic applications is the field of vehicle-manipulators, which are composed of a vehicle platform and a manipulator (robotic arm). The analysis and control of such systems has been studied extensively lately, and is providing promising new results in control tasks, trajectory optimization and redundancy resolution. The first applications of modelling of vehicle-manipulators in the literature are from the early 1990s [1] [2] [3] [4]. They focused on planning, controlling and the redundancy resolution of the configuration of the overall system. Since the year 2000, an even greater research effort was concentrated on simulating, controlling and building small vehicle-manipulators [5] [6]. There are general, singularity-free dynamic approaches [7] [8] [9] [10] and also other, more practical modelling techniques. One of the main focuses of these control algorithms is the redundancy resolution of the robotic arm [11]. In [12], the planning of the robotic arm trajectories and the nonholonomic vehicle in a global frame is presented. A control algorithm for these linked *dual-trajectories* is implemented and tested. In [13], the prioritization of these dual-trajectories is discussed. In case, one of the two subsystems cannot track its reference trajectory, the control algorithm determines whether the vehicle or the robotic arm should fulfil its trajectory tracking task with higher priority. A practical realization is presented in [14], in which a dual-trajectory control of a wheelchair mounted robotic arm is simulated and implemented. In [11], the kinematic redundancy resolution is presented. A general inverse kinematic procedure is introduced with the help of the so called *redundancy parameters*. These parameters allow the reduction of a redundant robotic arm to a simple one. The computed configuration of the redundant arm is the result of an optimization problem.

Another domain is the analysis and control of large, hydraulic robotic manipulators [15] [16] [17]. Such applications are forestry cranes, backhoe or road maintenance machineries [18]. The hydraulic and electro-hydraulic actuation of such machines is used because of their robustness and good power-to-weight ratio, but they imply further challenges due to highly non-linear and complex system characteristics [15]. To handle these challenges effectively, a stable and accurate low-level position and force control is required. The identification and the characterization of these nonlinear components require deep understanding and knowledge. Another problem is determining appropriate sensors for these open-air applications, because the installation of rotational displacement sensors is not possible on hydraulic actors and other fragile sensors do not operate properly in rough working area [19]. In [20], a self levelling system for a large working arm with a hydraulic actuation is presented. In [19] and [21], the modelling, the control and the automation of large hydraulic cranes is discussed. In [22], a model-based approach is discussed for the feedback control and [23] presents a nonlinear model predictive control for hydraulic forestry cranes and shows a great oscillation reduction of the endmanipulator. In [24], different linear and nonlinear control methods are implemented and compared on a test-bench. The results show the necessity and the benefits of the nonlinear control theory for hydraulic manipulators. Reference [25] presents modeling and identification methods for hydraulic manipulators and provides validation with measurements on a test-bench. Among the very detailed and physically motivated models, there are minimal and reduced-order models for hydraulic machines [26] [27].

They allow characterizations of such systems with help of dynamic transfer functions.

In this paper, we present a new approach to handle control challenges of heavy vehicle-manipulators during moving tasks (see Fig. 1). We assume that the moving platform is a middle-sized heavy-duty vehicle or tractor. The robot is a large hydraulic outdoor working arm with slow, controlled system dynamics. The equations of motion for the control model are derived in a local coordinate system around the reference trajectories, in the so called Frenét-frame [28]. In such a path-local coordinate system, the lateral and orientation error of the manipulator and vehicle are required through on-board localization and no global technique (like GPS) is necessary. This technique is already applied in automotive control theory [29]. In [30], this approach for a special case of small indoor vehicle-manipulator is discussed, but not in a general perspective. The here presented approach can also be used for different arm configurations.

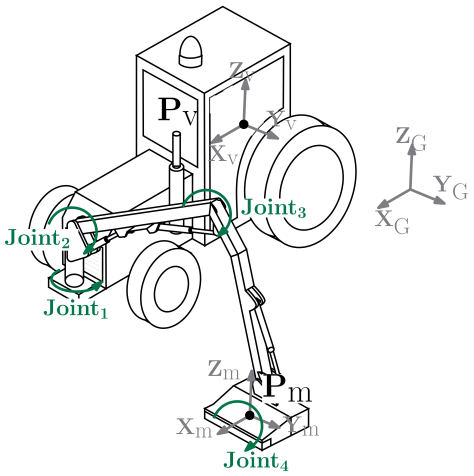

Fig. 1: Example for the overall system treating in this work

This paper has the following structure: section 2 presents a short description of the simulation environment for the vehicle and the robotic arm. In section 3, the proposed control model is discussed. The test-scenarios and the results of the control system are presented in section 4. In section 5, further challenges and research focuses are given.

II. Simulation environment

A. Vehicle model

A simulation environment is realized in Mathworks MATLAB/Simulink. The models of the chassis and the suspension system are based on [31]. The accuracy of the model is chosen to reproduce feasible vehicle motions for handling scenarios with lane keeping and trajectory following assistance. As the regarded working vehicles do not reach high velocities, a combined linear tire model is suitable for simulation. The implemented tire model is based on [32]. In [33] it has been shown that a simple modelling approach is suitable for testing and validating assistance functions for on- and off-road vehicles handling analysis.

B. Model of the robotic arm

The model of the working arm is set up with one rotary hydraulic joint and 3 hydraulic cylinders realizing the rotatory motions. The equations of motion of the arm are derived with Euler-Lagrange's equations of the second kind [34]. It is supposed that the hydraulic cylinders have third-order dynamics [27] [35]. This is a standard proposition for hydraulic systems actuated with fast directional control valves [17]. The parameters for the dead-zone and the transfer characteristics of the single joints are adapted from the literature [27]. The maximal angular speed of each single joints, which can be assumed for this application, is $\phi_i = 0.3$ rad/s. State feedback and gravity compensation deal with the nonlinearities [34]. For the trajectory tracking and modelling error compensation a slave PID controller is implemented with an additional feedforward term. The PID parameters are tuned empirically to have a good system response and to avoid strong overshoots. The inverse kinematic of the manipulator is derived analytically [36]. To determine the necessary joint angles for the desired position, the derivation uses the x_v, y_v, z_v coordinates of the end of the endeffector and the angle relative to the x_m-y_m plane. As a result, the high-level MPC is able to set the configuration of the robotic subsystem and the slave PID controller sets the desired position of the point P_m using the hydraulic cylinders.

III. Proposed control algorithm for vehicle-manipulator

A. Nonlinear model of the vehicle-manipulator

The proposed algorithm controls the vehicle manipulator in planar with a fixed horizontal position. The algorithm requires a control model of the overall system. Its characterisation happens through the following coordinate systems[1] (Fig. 2):

- a global frame O, index G
- frame of the rear axle of the vehicle at the point P_v, index v
- local frame on the reference trajectory Γ_v of the vehicle, around the point P_{rv}
- local frame on the reference trajectory Γ_m of the manipulator, around the point P_{rm}

Additionally the endpoint of the manipulator P_m is used for the derivation of the system dynamics. The equation of motion of the vehicle can be derived through the use of the velocity of the reference points P_v and P_m. The derivation for car-like vehicles is presented in [37]. The vehicle-manipulator are controlled by the steering angle of the vehicle δ, the projected length, a and by the orientation α of the robotic arm. For such a system a generalization can be introduced. Defining the variables s, d and $\Delta\theta$ for the vehicle (index v) and for the manipulator (index m):

- s_v and s_m are the curvilinear abscissas at the points P_{rv} and P_{rm} obtained by projecting P_v and P_m orthogonally on Γ_v and Γ_m. These points are unique if the point-pairs are close enough to each other.

[1]Note that the unit vectors are marked as $\mathbf{i}$ and $\mathbf{j}$ instead of $\mathbf{x}$ and $\mathbf{y}$ to avoid confusion with the latter system states.

- d_v and d_m are the lateral displacement from the reference trajectory of the vehicle and the manipulator in m. They are expressed in the orthonormal basis of the reference trajectories at the points $\mathrm{P_v}$ and $\mathrm{P_m}$.
- $\Delta\theta_\mathrm{v}$ is the orientation error of the vehicle in radian, $\Delta\theta_\mathrm{v} = \theta_\mathrm{v} - \theta_\mathrm{rv}$
- and $\Delta\theta_\mathrm{m}$ is the *manipulator's transformation angle* from end-manipulator's frame to the vehicle's frame in radian, $\Delta\theta_\mathrm{m} = \theta_\mathrm{v} - \theta_\mathrm{rm}$.
- The variable v without any index is the velocity of the rear axle of the vehicle in $\mathrm{m/s}$ which is necessary for the further derivation.
- The reference trajectories are described through their curvature, κ_rv and κ_rm in $1/\mathrm{m}$.

The bicycle model is given according to [37]:

$$\begin{aligned} \dot{s}_\mathrm{v} &= \frac{v}{1-\kappa_\mathrm{rv}\cdot d_\mathrm{v}}\cos(\Delta\theta_\mathrm{v}) \\ \dot{d}_\mathrm{v} &= v\sin(\Delta\theta_\mathrm{v}) \\ \Delta\dot{\theta}_\mathrm{v} &= v\frac{\tan(\delta)}{L} - \dot{s}_\mathrm{v}\kappa_\mathrm{rv} \end{aligned} \tag{1}$$

The idea of joint-dependent variables (a and α) can be found in some earlier works [13] [38], but only for small indoor robots in global frame for task priority redundancy resolution or dual-trajectory control.

Through the derivation of the manipulator dynamic in the Frenét-frame, $\dot{s}_\mathrm{m}$, $\dot{d}_\mathrm{m}$ and $\Delta\dot{\theta}_\mathrm{m}$ are determined. The curvature of e.g. Γ_m at the point $\mathrm{P_{rm}}$ is defined as $\kappa_\mathrm{rm} = \partial\theta_\mathrm{rm}/\partial s_\mathrm{m}$. This definition yields after substituting the time derivation of the manipulator's transformation angle

$$\Delta\dot{\theta}_\mathrm{m} = \dot{\theta}_\mathrm{v} - \dot{\theta}_\mathrm{rm} = \dot{\theta}_\mathrm{v} - \kappa_\mathrm{rm}\dot{s}_\mathrm{rm}. \tag{2}$$

Secondly, the position of $\mathrm{P_m}$ in the global frame $\mathbf{O}$ is required:

$$\overrightarrow{\mathrm{OP}}_\mathrm{m} = \overrightarrow{\mathrm{OP}}_\mathrm{v} + ((L+l) + a\cos\alpha)\,\mathbf{i}_\mathrm{v} + a\sin\alpha\,\mathbf{j}_\mathrm{v}. \tag{3}$$

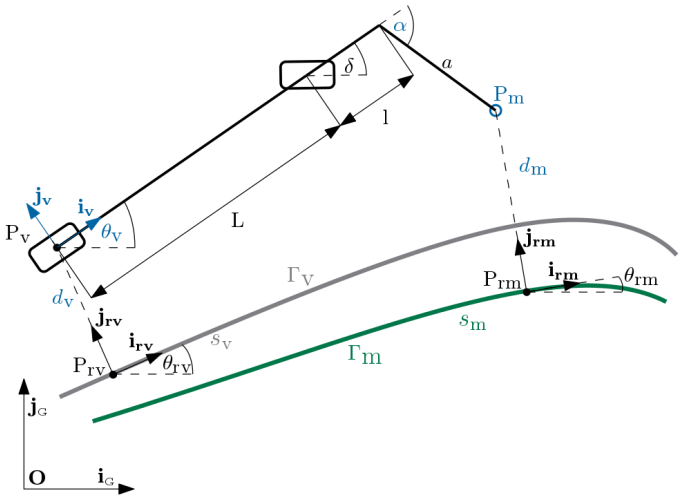

Fig. 2: The control model for the prediction of the manipulator's motion

With respect to the reference trajectory of the manipulator, $\overrightarrow{\mathrm{OP}}_\mathrm{m}$ is alternatively computed as

$$\overrightarrow{\mathrm{OP}}_\mathrm{m} = \overrightarrow{\mathrm{OP}}_\mathrm{rm} + d_\mathrm{m}\,\mathbf{j}_\mathrm{rm} \tag{4}$$

and the time-derivation of (3) is

$$\begin{aligned} \frac{\partial\overrightarrow{\mathrm{OP}}_\mathrm{m}}{\partial t} &= \frac{\partial\overrightarrow{\mathrm{OP}}_\mathrm{v}}{\partial t} + (L+l)\frac{\partial\,\mathbf{i}_\mathrm{v}}{\partial t} + (\dot{a}\cos\alpha - a\dot{\alpha}\sin\alpha)\;\mathbf{i}_\mathrm{v} \\ &\quad + a\cos\alpha\frac{\partial\,\mathbf{i}_\mathrm{v}}{\partial t} + (\dot{a}\sin\alpha + a\dot{\alpha}\cos\alpha)\;\mathbf{j}_\mathrm{v} \\ &\quad + a\sin\alpha\frac{\partial\,\mathbf{j}_\mathrm{v}}{\partial\,t}. \end{aligned} \tag{5}$$

With the substitution of $\frac{\partial\,\mathbf{i}_\mathrm{v}}{\partial\,t} = \dot{\theta}_\mathrm{v}\,\mathbf{j}_\mathrm{v}$, $\frac{\partial\,\mathbf{j}_\mathrm{v}}{\partial\,t} = -\dot{\theta}_\mathrm{v}\,\mathbf{i}_\mathrm{v}$ and $\frac{\partial\overrightarrow{\mathrm{OP}}_\mathrm{v}}{\partial\,t} = v\,\mathbf{i}_\mathrm{v}$ the equation of motion (5) is

$$\begin{aligned} \frac{\partial\overrightarrow{\mathrm{OP}}_\mathrm{m}}{\partial t} &= \Big(v + \dot{a}\cos\alpha - a(\dot{\theta}_\mathrm{v}+\dot{\alpha})\sin\alpha\Big)\;\mathbf{i}_\mathrm{v} \\ &\quad + \Big((L+l)\dot{\theta}_\mathrm{v} + \dot{a}\sin\alpha + a\cos\alpha(\dot{\theta}_\mathrm{v}+\dot{\alpha})\Big)\;\mathbf{j}_\mathrm{v}. \end{aligned} \tag{6}$$

The same velocity is computed from the reference trajectory of the manipulator in (4)

$$\begin{aligned} \frac{\partial\overrightarrow{\mathrm{OP}}_\mathrm{m}}{\partial t} &= \frac{\partial\overrightarrow{\mathrm{OP}}_\mathrm{rm}}{\partial t} + \frac{\partial}{\partial t}\left(d_\mathrm{m}\,\mathbf{j}_\mathrm{rm}\right) \\ &= \dot{s}_\mathrm{m}(1 - d_\mathrm{m}\kappa_\mathrm{rm})\,\mathbf{i}_\mathrm{rm} + \dot{d}_\mathrm{m}\,\mathbf{j}_\mathrm{rm}. \end{aligned} \tag{7}$$

Assuming $d_\mathrm{m}\cdot\kappa_{rm} \ll 1$ and transforming the manipulator's path coordinate system to the vehicle coordinate system, the dynamics of the manipulator is identified in the terms of equation (7) and equation (6) as follows:

$$\begin{aligned} \dot{s}_\mathrm{m} &= \cos\Delta\theta_\mathrm{m}\Big(v + \dot{a}\cos\alpha - a\dot{\alpha}\cos\alpha - a\dot{\theta}_\mathrm{v}\sin\alpha\Big) \\ &\quad - \sin\Delta\theta_\mathrm{m}\Big((L+l)\dot{\theta}_\mathrm{v} + a\dot{\theta}_\mathrm{v}\cos\alpha + \dot{a}\sin\alpha + a\dot{\alpha}\cos\alpha\Big) \end{aligned} \tag{8}$$

and

$$\begin{aligned} \dot{d}_\mathrm{m} &= \sin\Delta\theta_\mathrm{m}\Big(v + \dot{a}\cos\alpha - a\dot{\alpha}\cos\alpha - a\dot{\theta}_\mathrm{v}\sin\alpha\Big) \\ &\quad + \cos\Delta\theta_\mathrm{m}\Big((L+l)\dot{\theta}_\mathrm{v} + a\dot{\theta}_\mathrm{v}\cos\alpha + \dot{a}\sin\alpha + a\dot{\alpha}\cos\alpha\Big). \end{aligned} \tag{9}$$

Substituting (8) in the equation (2), the manipulator's transformation angle is

$$\begin{aligned} \Delta\dot{\theta}_\mathrm{m} = \kappa_\mathrm{rm}\Big[&\cos\Delta\theta_\mathrm{m}\Big(v + \dot{a}\cos\alpha - a\dot{\alpha}\cos\alpha - a\dot{\theta}_\mathrm{v}\sin\alpha\Big) \\ &- \sin\Delta\theta_\mathrm{m}\Big((L+l)\dot{\theta}_\mathrm{v} + a\dot{\theta}_\mathrm{v}\cos\alpha \\ &+ \dot{a}\sin\alpha + a\dot{\alpha}\cos\alpha\Big)\Big]. \end{aligned} \tag{10}$$

The equations (1), (8), (9) and (2) are used as the state space equation of the dynamic system.

B. Linear state-space model

For a computationally effective prediction, it is fundamental to have a linear model, which enables fast matrix computations. For that, the input *vehicle's curvature* is introduced from (1), $\kappa_\mathrm{v} = \frac{\tan(\delta)}{L}$. Thereby the input vector is

$$\mathbf{u}(t) = [\kappa_\mathrm{v}\ \dot{a}\ \dot{\alpha}]^T \tag{11}$$

where $\dot{a}$ and $\dot{\alpha}$ are the changing rates of the length and the angle of the manipulator. The state vector is chosen to

$$\mathbf{x}(t) = [d_\mathrm{v}\ \Delta\theta_\mathrm{v}\ d_\mathrm{m}\ \Delta\theta_\mathrm{m}\ a\ \alpha\ \kappa_\mathrm{rv}\ \kappa_\mathrm{rm}\ ]^T. \tag{12}$$

where κ_rv and κ_rm are the curvatures of the vehicle (index v) and of the manipulator (index m) reference trajectories. Their changing rates constitute the disturbance vector

$$\mathbf{z}(t) = [\dot{\kappa}_\mathrm{rv}\ \dot{\kappa}_\mathrm{rm}]^T. \tag{13}$$

It is assumed that the vehicle and the robotic manipulator move close along the reference trajectory (orientation errors $\Delta\theta_\mathrm{i} < 20^\circ$ and the lateral displacement $d_\mathrm{i} < R$, with $R = 1/\kappa_\mathrm{ri}$ the radius of the curve[2]). In that case, it is possible to linearize the trigonometrical functions and to assume that $\dot{s} \approx v$. The chosen operating point for the manipulator is

$$\begin{aligned}\mathbf{x}_0 &= [\ d_{\mathrm{v}0}\ \Delta\theta_{\mathrm{v}0}\ d_{\mathrm{m}0}\ \Delta\theta_{\mathrm{m}0}\ a_0\ \alpha_0\ \kappa_{\mathrm{rv}0}\ \kappa_{\mathrm{rm}0}\ ]^T \\ &= [\ 0\quad 0\quad 0\quad 0\quad a_e\ \alpha_e\quad 0\quad 0\ ]^T\end{aligned} \tag{14}$$

and

$$\begin{aligned}\mathbf{u}_0 &= [0\ 0\ 0]^T \\ \mathbf{z}_0 &= [0\ 0]^T.\end{aligned} \tag{15}$$

The linearization leads to the following time-variant state-space model:

$$\dot{\mathbf{x}}(t) = \mathbf{A}(t)\Delta\,\mathbf{x}(t) + \mathbf{B}(t)\Delta\,\mathbf{u}(t) + \mathbf{Z}\Delta\,\mathbf{z}(t), \tag{16}$$

with the perturbation around the equilibrium $\Delta\mathbf{x} = \mathbf{x} - \mathbf{x}_0$, $\Delta\mathbf{u} = \mathbf{u} - \mathbf{u}_0$ and $\Delta\mathbf{z} = \mathbf{z} - \mathbf{z}_0$. The used matrices are

$$\mathbf{A} = \begin{bmatrix} 0 & v & 0 & 0 & 0 & 0 & 0 & 0 \\ 0 & 0 & 0 & 0 & 0 & 0 & -v & 0 \\ 0 & 0 & 0 & v & 0 & 0 & 0 & 0 \\ 0 & 0 & 0 & 0 & 0 & 0 & 0 & -v \\ 0 & 0 & 0 & 0 & 0 & 0 & 0 & 0 \\ 0 & 0 & 0 & 0 & 0 & 0 & 0 & 0 \\ 0 & 0 & 0 & 0 & 0 & 0 & 0 & 0 \\ 0 & 0 & 0 & 0 & 0 & 0 & 0 & 0 \end{bmatrix}, \tag{17}$$

$$\mathbf{B} = \begin{bmatrix} 0 & 0 & 0 \\ v & 0 & 0 \\ (L + l + a_e\cos\alpha_e)v & \sin\alpha_e & a_e\cos\alpha_e \\ v & 0 & 0 \\ 0 & 1 & 0 \\ 0 & 0 & 1 \\ 0 & 0 & 0 \\ 0 & 0 & 0 \end{bmatrix} \tag{18}$$

[2]The index $i = v, m$

and

$$\mathbf{Z} = \begin{bmatrix} 0 & 0 & 0 & 0 & 0 & 0 & 1 & 0 \\ 0 & 0 & 0 & 0 & 0 & 0 & 0 & 1 \end{bmatrix}^T. \tag{19}$$

Note that the parameters v, a_e and α_e are time varying. They are updated in each prediction sequence.
Four values are used as outputs of the system:

- the flat output d_v of the vehicle dynamics
- the lateral error on the front axle of the vehicle dynamics, $d_\mathrm{v} + (L + l)\sin(\Delta\theta)$
- the lateral error of manipulator d_m
- the length of the manipulator a.

They are necessary to handle the constraints. Assuming $\sin(\Delta\theta) \approx \Delta\theta$, the linear output equation is

$$\mathbf{y} = \mathbf{C}\,\mathbf{x} \tag{20}$$

with

$$\mathbf{C} = \begin{bmatrix} 1 & 0 & 0 & 0 & 0 & 0 & 0 & 0 \\ 1 & L + l & 0 & 0 & 0 & 0 & 0 & 0 \\ 0 & 0 & 1 & 0 & 0 & 0 & 0 & 0 \\ 0 & 0 & 0 & 0 & 1 & 0 & 0 & 0 \end{bmatrix}. \tag{21}$$

C. Time-varying time-discrete model

The continuous-time system is transformed into a discrete-time representation to provide a suitable description for the prediction procedure. For each time step, constant state, input, and output matrices, as well as piecewise constant control inputs and disturbances are accounted form. The temporal discretization is performed by using zero-order hold elements with the sampling time T [39]:

$$\begin{aligned}\mathbf{A}_\mathrm{d} &= e^{\mathbf{A}T},\ \ \mathbf{B}_\mathrm{d} = \int_0^T e^{\mathbf{A}\tau}\,\mathrm{d}\tau\cdot\mathbf{B} \\ \mathbf{C}_\mathrm{d} &= \mathbf{C},\quad \mathbf{Z}_\mathrm{d} = \int_0^T e^{\mathbf{A}\tau}\,\mathrm{d}\tau\cdot\mathbf{Z}.\end{aligned} \tag{22}$$

The disturbance changing rate is computed with a discrete forward-euler first order derivative.

D. Cost function and constraints

The cost function of the optimization can be formulated as quadratic function for N prediction steps:

$$J(\mathbf{x}(t), \mathbf{u}(t)) = \sum_{i=0}^{\mathrm{N}} \mathbf{x}_\mathrm{i}^T\mathbf{Q}_\mathrm{i}\,\mathbf{x}_\mathrm{i} + \sum_{i=0}^{\mathrm{N}} \mathbf{u}_\mathrm{i}^T\mathbf{R}_\mathrm{i}\,\mathbf{u}_\mathrm{i}, \tag{23}$$

with

$$\mathbf{Q}_\mathrm{i} = \begin{bmatrix} G_{d_\mathrm{v}} & 0 & 0 & 0 & 0 & 0 & 0 & 0 \\ 0 & G_{\Delta\theta_\mathrm{v}} & 0 & 0 & 0 & 0 & 0 & 0 \\ 0 & 0 & G_{d_\mathrm{m}} & 0 & 0 & 0 & 0 & 0 \\ 0 & 0 & 0 & 0 & 0 & 0 & 0 & 0 \\ 0 & 0 & 0 & 0 & 0 & 0 & 0 & 0 \\ 0 & 0 & 0 & 0 & 0 & G_{\Delta\alpha} & 0 & 0 \\ 0 & 0 & 0 & 0 & 0 & 0 & 0 & 0 \\ 0 & 0 & 0 & 0 & 0 & 0 & 0 & 0 \end{bmatrix} \tag{24}$$

and

$$\mathbf{R}_{\mathrm{i}} = \begin{bmatrix} G_{\kappa_{\mathrm{v}}} & 0 & 0 \\ 0 & G_{\dot{a}} & 0 \\ 0 & 0 & G_{\dot{\alpha}} \end{bmatrix} \tag{25}$$

In accordance with the objective of the control algorithm, the weights of the quadratic cost function need to be chosen with respect of the following points:

- G_d and $G_{\Delta\theta}$ are required for a smooth lane keeping
- $G_{\kappa_{\mathrm{v}}}$ penalizes the vehicle's curvature
- $G_{d_{\mathrm{m}}}$ and $G_{\Delta\alpha}$ are necessary for a smooth control of the manipulator
- the curvature of the reference trajectories κ_{rv} and κ_{rm} are not penalized, as they are only necessary for a good system description
- a and $\Delta\theta_{\mathrm{m}}$ are not penalized, they are only considered through the output equation to ensure the constraints
- the inputs $\dot{a}$ and $\dot{\alpha}$ are penalized to get a feasible and smooth motion.

Through adjusting the above-mentioned parameters, the priority of the dual-trajectories can be changed.

Obstacles on the manipulator working space, road side or other objects are treated as constraints of the optimization problem. Constraints are necessary for

- the inputs $\dot{a}$ and $\dot{\alpha}$, by the reason of the slow dynamics of the robotic arm and the steering actuator

$$\begin{aligned} \dot{a}_{\mathrm{min}} \leq \dot{a} \leq \dot{a}_{\mathrm{max}} \\ \dot{\alpha}_{\mathrm{min}} \leq \dot{\alpha} \leq \dot{\alpha}_{\mathrm{max}} \end{aligned} \tag{26}$$

- the length a due to the maximal and minimal configuration of the manipulator

$$a_{\mathrm{min}} \leq a \leq a_{\mathrm{max}} \tag{27}$$

- the vehicle curvature κ_v according to the steering system on the vehicle
- the vehicle system states due to the roadside
- the lateral error d_{m} of the robotic arm to treat the static and dynamic obstacles on the working space.

E. Linear quadratic optimization problem

To formulate a linear quadratic optimization problem, the future system states are computed as function of the input sequence. This can be done with the help of the so called batch approach [40] [41]. Using the prediction model, the cost function and the constraints, it is possible to set up a constrained linear quadratic optimization problem, which can be solved effectively with QP-solvers. The future system states $\mathbf{x}_s$ and outputs $\mathbf{y}_s$ computed by use of the future disturbances-sequence $\mathbf{z}_s$, input-sequences $\mathbf{u}_s$ and the initial system states $\mathbf{x}_0$ for N prediction steps[3]

$$\mathbf{x}_s = \mathcal{A}\,\mathbf{x}_0 + \mathcal{B}\,\mathbf{u}_s + \mathcal{Z}\,\mathbf{z}_s. \tag{28}$$

[3]For the sake of simplicity the index s is used for the vector sequences: $\mathbf{x}_s = [\,\mathbf{x}(1),\ \mathbf{x}(2)\ \ldots\ \mathbf{x}(N)]^T$ for the future system states, $\mathbf{y}_s = [\,\mathbf{y}(1),\ \mathbf{y}(2)\ \ldots\ \mathbf{y}(N)]^T$ for the future system outputs, $\mathbf{z}_s = [\,\mathbf{z}(0),\ \mathbf{z}(1)\ \ldots\ \mathbf{z}(N-1)]^T$ for the future curvature changing and $\mathbf{u}_s = [\,\mathbf{u}(0),\ \mathbf{u}(1)\ \ldots\ \mathbf{u}(N-1)]^T$ for the optimizing future inputs.

The used matrices are

$$\mathcal{A} = \begin{bmatrix} \mathbf{A} \\ \mathbf{A}^2 \\ \vdots \\ \mathbf{A}^N \end{bmatrix}, \tag{29}$$

$$\mathcal{B} = \begin{bmatrix} \mathbf{B} & \mathbf{0} & \ldots & \mathbf{0} \\ \mathbf{AB} & \mathbf{B} & \ldots & \mathbf{0} \\ \vdots & \ddots & \ddots & \vdots \\ \mathbf{A}^{N-1}\mathbf{B} & \ldots & \mathbf{AB} & \mathbf{B} \end{bmatrix} \tag{30}$$

and

$$\mathcal{Z} = \begin{bmatrix} \mathbf{Z} & \mathbf{0} & \ldots & \mathbf{0} \\ \mathbf{AZ} & \mathbf{Z} & \ldots & \mathbf{0} \\ \vdots & \ddots & \ddots & \vdots \\ \mathbf{A}^{N-1}\mathbf{Z} & \ldots & \mathbf{AZ} & \mathbf{B} \end{bmatrix}. \tag{31}$$

The output matrix is

$$\mathcal{C} = \mathrm{diag}[\mathbf{C}\ \ldots\ \mathbf{C}], \tag{32}$$

so that the future output sequence is

$$\mathbf{y}_s = \mathcal{C}\,(\mathcal{A}\,\mathbf{x}_0 + \mathcal{B}\,\mathbf{u}_s + \mathcal{Z}\,\mathbf{z}_s)\,. \tag{33}$$

By applying the system state and output sequence (28) and (33), the cost function is formed depending on the input sequence $\mathbf{u}_s$

$$J(\mathbf{u}_s) = \mathbf{u}_s^T\mathcal{H}\,\mathbf{u}_s + 2\left(\mathbf{x}_0\mathcal{F} + \mathbf{z}^T\mathcal{Y}\right)\mathbf{u}_s + K. \tag{34}$$

with $\mathcal{H} = \mathcal{B}^T\mathcal{Q}\mathcal{B}+\mathcal{R}$, $\mathcal{F} = \mathcal{A}^T\mathcal{Q}\mathcal{B}$ and $\mathcal{Y} = \mathcal{Z}^T\mathcal{Q}\mathcal{B}$. The constant term K does not influence the optimal control sequence. The constraints from subsection III-D can be expressed with help of (33) as $\mathbf{y}_{\mathrm{min}}$ and $\mathbf{y}_{\mathrm{max}}$. This may be reformulated in terms of $\mathbf{u}_s$

$$\begin{bmatrix} \mathcal{C}\mathcal{B} \\ -\mathcal{C}\mathcal{B} \end{bmatrix}\mathbf{u}_s \leq \begin{bmatrix} \mathbf{y}_{\mathrm{max}} - \mathcal{C}\mathcal{A}\,\mathbf{x}_0 \\ -\mathbf{y}_{\mathrm{min}} + \mathcal{C}\mathcal{A}\,\mathbf{x}_0 \end{bmatrix}. \tag{35}$$

The resulting quadratic optimization problem - minimizing the cost function (34) under the constraints (26) and (35) - can be solved by standard numerical QP-solvers.
An iterative solution is provided here by the interior-point method for convex problems [42].

IV. Test scenarios and simulation results

Based on two predefined scenarios the control algorithm is tested and validated. The simulations are carried out with Mathworks MATLAB/Simulink, with $dt_{\mathrm{sim}} = 0.5$ ms fixed step simulation time and Runge-Kutta solver. The number of prediction steps is chosen to $N = 10$ and the sampling-time is set to $T_{\mathrm{pred}} = 0.1$ s. The constraints for the manipulator are $\dot{a}_{\mathrm{max}} = 0.025$ m/s, $\dot{a}_{\mathrm{min}} = -\dot{a}_{\mathrm{max}}$, $\dot{\alpha}_{\mathrm{max}} = 0.02\ \frac{\mathrm{rad}}{\mathrm{s}}$ and $\dot{\alpha}_{\mathrm{min}} = -\dot{\alpha}_{\mathrm{max}}$. The schematic representation of the simulation environment is shown in Fig. 3. The MPC only needs the reference points for the configuration of the robotic arm, α_e and a_e, because the other elements of the state-space vector

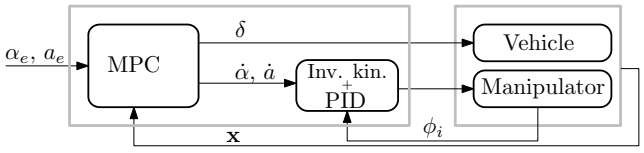

Fig. 3: Block representation of the simulation and control

x are defined the errors, meaning they do not need reference signals (compare with equation 14).

The first scenario (see Fig. 4) starts with an initial orientation and lateral error both for the vehicle and working arm. After reaching the steady-state straight ahead motion a double position change for the working arm is performed. During the lane change the vehicle supports the motion of the robotic arm by deviating from its desired trajectory between $x = 25$ m and $x = 35$ m as well as between $x = 55$ m and $x = 75$ m. In the second setting, the priorities are changed

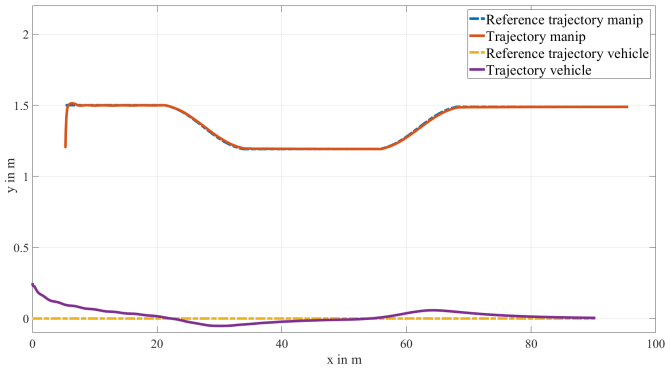

Fig. 4: Scenario 1, setting 1 - motions of the overall system with vehicle motion support

by adjusting the penalty weights. The vehicle motion has now a higher priority and does not support the robotic arm, the deviation is smaller than above (see Fig 5). The second

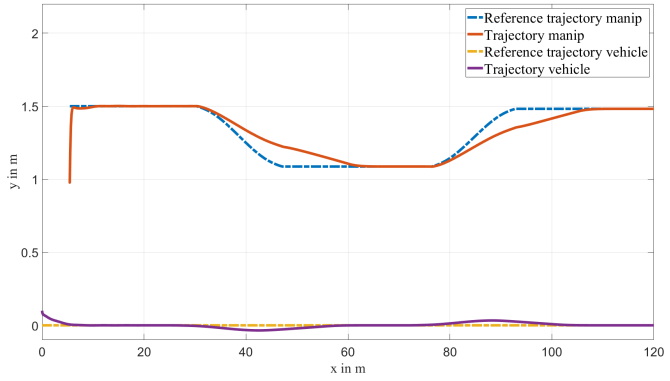

Fig. 5: Scenario 1, setting 2 - motions of the overall system without vehicle motion support

scenario is a left curve (see Fig 6). After reaching the steady-state cornering, the trajectory must be re-planned due to an obstacle in the work-space of the manipulator. This obstacle is represented by an additional constraint of the optimization problem. The algorithm is capable of changing the trajectories smoothly. Note that the modified trajectories are optimized through the weights of the cost function (23) assigning a higher priority to the robotic arm, so the vehicle assists the motion of the manipulator. The selected scenarios show that

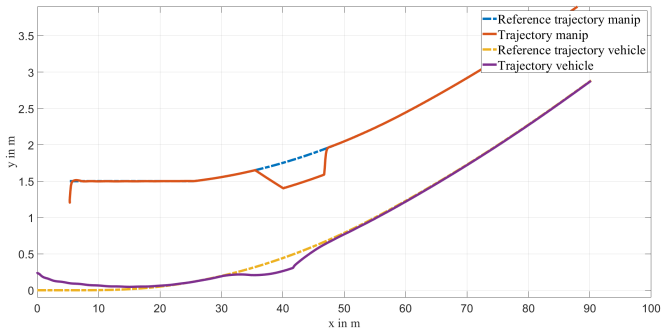

Fig. 6: Scenario 2 - trajectory re-planning due to constraints

the control algorithm is able to control the overall system from initial errors into a steady state motion. It can follow reference trajectory with changing curvature and it can re-plan the trajectories smoothly due to active constraints.

V. Conclusion and Future Research

In this paper a new approach for control and trajectory optimization of large vehicle manipulators is presented. The system equations of the control model are introduced in the so-called Frenét-frame, as a generalization of the equations of motion in a global coordinate system. The main idea is to use a model, consisting a 2 DoF robotic arm and a bicycle model, to describe and predict the motion of the overall system in planar. The applied MPC operates in a path-local coordinate system and no global localization is required. A simulation environment is implemented in MATLAB/Simulink for tests and validation. A slave control loop regulates each hydraulic joint according to the high-level MPC controller. The control problem is formulated as linear quadratic optimization problem using the prediction model, constraints and a cost function. The dynamics of the overall system are taken into account by the constraints. Collisions with obstacles on the robot's working area may be avoided by including them in the constraints, leading to re-plan the dual-trajectories for the same curvature input. A prioritization between the trajectories can be done by adjusting the penalty parameters of the cost function. The control technique has been tested and validated in simulations by two predefined scenarios.

Future works will focus on the extension of the cost function with the configuration of a more complex robotic arm. For such a robotic arm, the redundancy resolution can be an important aspect. Another focus is to find a suitable description of the system for 3D motions. Analysis and control of the vehicle motion to reduce the dynamic influences on the driver is also an important aspect. For real

applications, the robustness of this control structure should be discussed. Sensors and other measurement instruments will be modelled too.

REFERENCES

[1] S. Dubowsky and E. Vance, "Planning mobile manipulator motions considering vehicle dynamic stability constraints," in *Proceedings, 1989 International Conference on Robotics and Automation*. IEEE Comput. Soc. Press, 1989.

[2] Y. Yamamoto and X. Yun, "Coordinating locomotion and manipulation of a mobile manipulator," *IEEE Transactions on Automatic Control*, vol. 39, no. 6, pp. 1326–1332, 1994.

[3] K. Liu and F. Lewis, "Decentralized continuous robust controller for mobile robots," in *Proceedings., IEEE International Conference on Robotics and Automation*. IEEE Comput. Soc. Press, 1990.

[4] H. Seraji, "A unified approach to motion control of mobile manipulators," *The International Journal of Robotics Research*, vol. 17, no. 2, pp. 107–118, 1998.

[5] G. D. White, R. M. Bhatt, and V. N. Krovi, "Dynamic redundancy resolution in a nonholonomic wheeled mobile manipulator," *Robotica*, vol. 25, no. 02, 2007.

[6] Z. Li, A. Ming, N. Xi, and M. Shimojo, "Motion control of nonholonomic mobile underactuated manipulator," in *Proceedings 2006 IEEE International Conference on Robotics and Automation, 2006. ICRA 2006.* IEEE, 2006.

[7] V. Duindam and S. Stramigioli, "Lagrangian dynamics of open multibody systems with generalized holonomic and nonholonomic joints," in *2007 IEEE/RSJ International Conference on Intelligent Robots and Systems*. IEEE, 2007.

[8] V. Duindam and S. Stramigioli, "Singularity-free dynamic equations of open-chain mechanisms with general holonomic and nonholonomic joints," *IEEE Transactions on Robotics*, vol. 24, no. 3, pp. 517–526, 2008.

[9] P. J. From, "An explicit formulation of singularity-free dynamic equations of mechanical systems in lagrangian form—part one: Single rigid bodies," *Modeling, Identification and Control: A Norwegian Research Bulletin*, vol. 33, no. 2, pp. 45–60, 2012.

[10] P. J. From, "An explicit formulation of singularity-free dynamic equations of mechanical systems in lagrangian form—part two: Multibody systems," *Modeling, Identification and Control: A Norwegian Research Bulletin*, vol. 33, no. 2, pp. 61–68, 2012.

[11] R. Ancona, "Redundancy modelling and resolution for robotic mobile manipulators: a general approach," *Advanced Robotics*, vol. 31, no. 13, pp. 706–715, 2017.

[12] G. D. White, R. M. Bhatt, C. P. Tang, and V. N. Krovi, "Experimental evaluation of dynamic redundancy resolution in a nonholonomic wheeled mobile manipulator," *IEEE/ASME Transactions on Mechatronics*, vol. 14, no. 3, pp. 349–357, 2009.

[13] M. Mashali, R. Alqasemi, and R. Dubey, "Task priority based dual-trajectory control for redundant mobile manipulators," in *2014 IEEE International Conference on Robotics and Biomimetics (ROBIO 2014)*. IEEE, 2014.

[14] M. Mashali, R. Alqasemi, S. Sarkar, and R. Dubey, "Design, implementation and evaluation of a motion control scheme for mobile platforms with high uncertainties," in *5th IEEE RAS/EMBS International Conference on Biomedical Robotics and Biomechatronics*. IEEE, 2014.

[15] J. Mattila, J. Koivumaki, D. G. Caldwell, and C. Semini, "A survey on control of hydraulic robotic manipulators with projection to future trends," *IEEE/ASME Transactions on Mechatronics*, vol. 22, no. 2, pp. 669–680, 2017.

[16] M. Sirouspour and S. Salcudean, "Nonlinear control of hydraulic robots," *IEEE Transactions on Robotics and Automation*, vol. 17, no. 2, pp. 173–182, 2001.

[17] R. B. Walters, *Hydraulic and Electro-Hydraulic Control Systems*. Springer Netherlands, 1991.

[18] M. C. Bing Xu, "Motion control of multi-actuator hydraulic systems for mobile machineries: Recent advancements and future trends," *Frontiers of Mechanical Engineering*, no. Issue 2, pp. 151–166, 2018.

[19] P. L. Hera, U. Mettin, S. Westerberg, and A. Shiriaev, "Modeling and control of hydraulic rotary actuators used in forestry cranes," in *2009 IEEE International Conference on Robotics and Automation*. IEEE, 2009.

[20] I. Yung, C. Vázquez, and L. B. Freidovich, "Robust position control design for a cylinder in mobile hydraulics applications," *Control Engineering Practice*, vol. 69, pp. 36–49, 2017.

[21] S. Fodor, C. Vazquez, and L. Freidovich, "Automation of slewing motions for forestry cranes," in *2015 15th International Conference on Control, Automation and Systems (ICCAS)*. IEEE, 2015.

[22] P. L. Hera and D. O. Morales, "Model-based development of control systems for forestry cranes," *Journal of Control Science and Engineering*, vol. 2015, pp. 1–15, 2015.

[23] J. Kalmari, J. Backman, and A. Visala, "Nonlinear model predictive control of hydraulic forestry crane with automatic sway damping," *Computers and Electronics in Agriculture*, vol. 109, pp. 36–45, 2014.

[24] M. M. Bech, T. O. Andersen, H. C. Pedersen, and L. Schmidt, "Experimental evaluation of control strategies for hydraulic servo robot," in *2013 IEEE International Conference on Mechatronics and Automation*. IEEE, 2013.

[25] P. L. Hera, B. U. Rehman, and D. O. Morales, "Electro-hydraulically actuated forestry manipulator: Modeling and identification," in *2012 IEEE/RSJ International Conference on Intelligent Robots and Systems*. IEEE, 2012.

[26] M. Ruderman, "Minimal-model for robust control design of large-scale hydraulic machines," in *2018 IEEE 15th International Workshop on Advanced Motion Control (AMC)*. IEEE, 2018.

[27] M. Ruderman, "Full- and reduced-order model of hydraulic cylinder for motion control," in *IECON 2017 - 43rd Annual Conference of the IEEE Industrial Electronics Society*. IEEE, 2017.

[28] W. Kühnel, *Differential geometry: Curves - surfaces - manifolds*, third edition ed., ser. Student mathematical library. Providence, Rhode Island: American Mathematical Society, 2015, vol. volume 77.

[29] M. Werling, J. Ziegler, S. Kammel, and S. Thrun, "Optimal trajectory generation for dynamic street scenarios in a frenet frame," in *2010 IEEE International Conference on Robotics and Automation*. IEEE, 2010.

[30] A. Mazur and D. Szakiel, "On path following control of nonholonomic mobile manipulators," *International Journal of Applied Mathematics and Computer Science*, vol. 19, no. 4, pp. 561–574, 2009.

[31] R. L. Kovacs, L. Nadai, and Z. Hankovszki, "Modeling of commercial vehicles for vehicle dynamics control development," in *2014 IEEE 9th IEEE International Symposium on Applied Computational Intelligence and Informatics (SACI)*. IEEE, 2014.

[32] G. R. Georg (University of Applied Sciences, Regensburg, *Road Vehicle Dynamics*. Taylor & Francis Inc, 2011.

[33] O. Lindgärde and M. Gäfvert, "A 9-DOF tractor-semitrailer dynamic handling model for advanced chassis control studies," *Vehicle System Dynamics*, vol. 41, no. 1, pp. 51–82, 2004.

[34] F. C. P. Kevin M. Lynch, *Modern Robotics*. Cambridge University Press, 2017.

[35] M. H. Rudolfsen, T. N. Aune, O. Auklend, L. T. Aarland, and M. Ruderman, "Identification and control design for path tracking of hydraulic loader crane," in *2017 IEEE International Conference on Advanced Intelligent Mechatronics (AIM)*. IEEE, 2017.

[36] R. M. Murray, *A Mathematical Introduction to Robotic Manipulation*. CRC Press, 2017.

[37] O. K. Bruno Siciliano, Ed., *Springer Handbook of Robotics*. Springer International Publishing, 2008, ch. 34. Motion Control of wheeled mobile robots, p. pp. 803.

[38] M. Mashali, R. Alqasemi, and R. Dubey, "Mobile manipulator dual-trajectory tracking using control variables introduced to end-effector task vector," in *2016 World Automation Congress (WAC)*. IEEE, 2016.

[39] J. Lunze, *Regelungstechnik 2*. Springer Berlin Heidelberg, 2016.

[40] F. Borrelli, *Predictive Control for Linear and Hybrid Systems*. CAMBRIDGE UNIVERSITY PRESS, 2017.

[41] B. Gutjahr and M. Werling, "Optimale fahrzeugquerführung mittels linearer, zeitvarianter mpc," in *10. Workshop Fahrerassistenzsysteme - FAS 2015*. Uni-DAS e.V., 2015, pp. 61–70.

[42] S. W. Jorge Nocedal, *Numerical Optimization*. Springer New York, 2006.